

Displacement effect in strong-field atomic ionization by an XUV pulse

Igor A. Ivanov, Anatoli S. Kheifets, and Klaus Bartschat*

Research School of Physical Sciences, The Australian National University, Australian National University, Canberra, Australian Capital Territory 0200, Australia

John Emmons and Sean M. Buczek

Department of Physics and Astronomy, Drake University, Des Moines, Iowa 50311, USA

Elena V. Gryzlova and Alexei N. Grum-Grzhimailo

Skobeltsyn Institute of Nuclear Physics, Lomonosov Moscow State University, Moscow 119991, Russia

(Received 15 June 2014; published 3 October 2014)

We study strong-field atomic ionization driven by an XUV pulse with a nonzero displacement, the quantity defined as the time integral of the pulse vector potential taken over the pulse duration. The use of such pulses may lead to an extreme sensitivity of the ionization process to subtle changes of a driving XUV pulse, in particular, the ramp-on and off profile and the carrier envelope phase. We illustrate this sensitivity for atomic hydrogen and lithium driven by few-femtosecond XUV pulses with intensity in the $10^{14}\text{W}/\text{cm}^2$ range. The observed effect is general and should modify strong-field ionization of any atom or molecule, provided the ionization rate is sufficiently high.

DOI: [10.1103/PhysRevA.90.043401](https://doi.org/10.1103/PhysRevA.90.043401)

PACS number(s): 32.80.Rm, 32.80.Fb, 32.90.+a, 42.50.Hz

Over the past decade, it has become possible to generate short and intense pulses of coherent extreme ultraviolet (XUV) radiation. Subfemtosecond XUV pulses from high-order harmonic generation (HHG) sources [1,2] are widely used for time-resolved studies of atomic photoionization in attosecond streaking [3] and interferometric [4] experiments, while femtosecond pulses from free-electron lasers (FEL) [5,6] are instrumental for studying complex dynamics governing both sequential and direct multiple ionization processes [7].

There are certain peculiarities of the photoionization process in this short-wavelength intense-field regime. A nonresonant radiation field of high intensity can dress the single-electron continuum states, resulting in a distorted multipeak structure of the photoelectron spectra [8]. The multi peaked spectra are typically explained in terms of the dressed-state picture [9,10], or by dynamical interference in the emission process through the interplay between the photoionization and the ac Stark shift [11].

In this paper, we report yet another peculiarity of strong-field atomic ionization. Under a certain condition, the photoionization process becomes extremely sensitive to subtle changes of the driving XUV pulse such as the ramp-on and off profile and the carrier envelope phase (CEP). This condition can be formulated as a nonzero net displacement of the free electron, originally at rest, observed after the end of the pulse. The displacement is expressed as the time integral of the pulse vector potential calculated over the pulse duration. (We assume that the vector potential is zero before and after the pulse.) For nonzero displacement, seemingly insignificant changes of the pulse parameters may have a dramatic effect on the photoelectron spectrum and the photoelectron angular distribution (PAD).

We explain this effect within the Kramers-Henneberger (KH) picture of the ionization process, in which the so-called “KH atom” is moving in the reference frame of the ionized electron. The ionic potential seen by the photoelectron in this frame and averaged over its oscillations, known as the KH potential, is distinctly different from the original atomic potential, but still capable of supporting infinitely many bound states. These bound states can be imaged by photoelectron spectroscopy and are responsible for unexpected stabilization of atomic ionization by intense IR laser pulses [12]. A similar analysis of the KH potential was used to capture the most essential physics of strong-field atomic ionization [13]. In the present case, a hardly noticeable change of the ramp-on and off profile from linear to sine-squared of a long flat-top pulse results in dramatically different KH potentials. This, in turn, alters the entire photoionization process and results in a major variation of the photoelectron spectrum as well as the PAD.

To our knowledge, little attention has been paid to date to strong-field ionization driven by the pulses with a nonzero displacement. About 20 years ago, the possibility was discussed [14] but not followed through. In this paper we study ionization driven by such pulses for realistic scenarios and suggest a specific recipe for possible experimental tests.

We illustrate the ramp-on and off and CEP effects for hydrogen and lithium atoms driven by ~ 10 femtosecond pulses with peak intensity in the $10^{14}\text{W}/\text{cm}^2$ range. Even though we use specific XUV pulse parameters, the predicted effects appear to be general and should modify strong-field ionization of any atom or molecule, including resonant photoionization, provided the ionization rate is sufficiently high. All examples presented in this paper are for pulses with the electric field $\mathbf{E}(t) = F(t) \sin(\omega t + \delta) \hat{z}$ linearly polarized along the z direction. Here $F(t)$ is the envelope function, ω is the central frequency, and the CEP δ is usually (except for one case) chosen as zero.

We describe the photoionization process by the nonrelativistic time-dependent Schrödinger equation (TDSE), which

*Permanent Address: Department of Physics and Astronomy, Drake University, Des Moines, Iowa 50311, USA.

can be solved to a very high degree of accuracy. We ignore any nondipole, including magnetic field, effects. This is well justified for the chosen pulses. As shown in [15], the degree of adiabaticity of the laser-atom interaction does not modify significantly the breakdown of the dipole approximation. Furthermore, the criterion $F_0/c\omega^3 \ll 1$ [15], where F_0 is the field amplitude and c is the speed of light, is very well fulfilled in our calculations. The latter condition corresponds to a displacement of the electron due to the magnetic field by much less than the size of the initial wave packet.

For the numerical treatment, we employed either the length or velocity gauge of the electric dipole operator and three time-propagation schemes (Crank-Nicolson [16], matrix iteration [17], and short iterative Lanczos [18]). All these schemes and gauges produced essentially identical (within the thickness of the lines) results. For the laser pulses we consider, the matrix iteration method employing the velocity gauge provides the fastest and least computationally demanding way to solve the TDSE. In view of the unexpected character of our results, we employed the other schemes and gauges to ensure the correctness of our predictions. Exhaustive tests were performed to ensure numerical stability with respect to the space and time grids, as well as the number of partial waves coupled in the solution of the TDSE. For hydrogen, this stability and accuracy were used to calibrate the absolute laser intensity at the 1% level [19,20]. For lithium, a very accurate theoretical description of the experimental strong-field ionization spectra was also achieved [21].

As a convenient numerical example, we consider electric field pulses with envelope functions of trapezoidal (linear ramp-on and off) shape and sine-squared shape. Both functions have the numerical advantage that they start at true zero and are switched off completely within a finite (not necessarily integer) number of cycles. In addition, an extended plateau in the envelope function characterizes the amplitude of the electric field.

Figure 1 shows an example of two pulses, which we will denote by “2-36-2 *S-S*” and “2-36-2 *L-L*,” respectively. Here “ n_1 - n_2 - n_3 ” refers to the number of cycles in the ramp-on (n_1), the plateau (n_2), and the ramp-off (n_3), while “*S*” and “*L*” label sine-squared (*S*) or linear (*L*) ramp-on or off. In this particular example, the peak intensity is $4.0 \times 10^{14} \text{ W/cm}^2$, corresponding to a peak electric field amplitude of 0.107 atomic units (a.u.). The central photon energy is 19 eV (0.7 a.u.). A similar pulse was studied recently in the context of testing numerical approaches [22,23], except that the central photon frequency was chosen to coincide with the nonrelativistic $1s$ - $2p$ resonance transition energy. We chose a nonresonant frequency significantly larger than the field-free ionization potential in the present work to avoid the impression that the effects discussed below are limited to particular resonant cases.

While the well-known multiphoton character in the ejected-electron energy spectrum displayed on a logarithmic scale in Fig. 2 may not look peculiar at all, the *insets* show that the ramp-on and off effect can be substantial. It not only depends on how the pulse is switched on and off within a given number of optical cycles (o.c.), but also on how many cycles are taken for the on and off steps. Specifically, the dominant single-photon peak displayed in the insets changes its height and width when comparing the two 2-36-2 pulses, while virtually

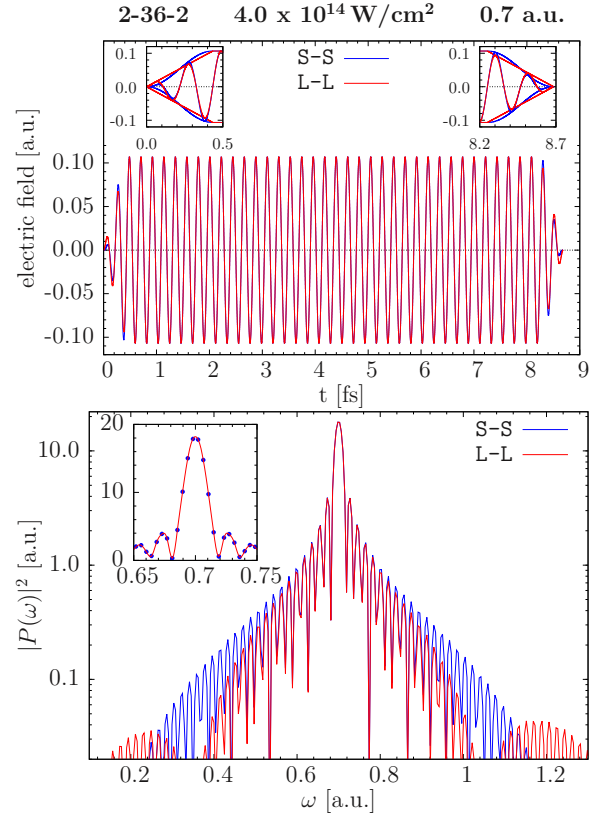


FIG. 1. (Color online) Electric field (top) and Fourier spectrum (bottom) of 2-36-2 *L-L* and *S-S* pulses with central photon energy 0.7 a.u. and peak intensity $4.0 \times 10^{14} \text{ W/cm}^2$. The insets magnify the changes due to the small differences in the ramp-on and off cycles. The pulses are identical in the plateau regime.

no difference occurs for 1.5-37-1.5. Other peaks at higher photoelectron energies, corresponding to absorption of two and three photons, are split into doublets. These results may seem surprising, as both the *L-L* and *S-S* pulses have very similar spectral content as is seen on the bottom panel of Fig. 1.

Further analysis revealed that not only the angle-integrated spectra are very sensitive to the ramp-on or off. The partial-wave decomposition of the ionization probability, for example, and the evolution of the expectation value $\langle L^2 \rangle$ as function of time, are completely different for the 2-36-2 *S-S* and 2-36-2 *L-L* pulses (see Fig. 3). While the $\langle L^2 \rangle$ expectation value in the presence of the laser pulse is not a directly observable quantity (it is not gauge invariant: the bottom panel of Fig. 3 illustrates its evolution if the velocity gauge is employed), the marked difference in its behavior for 2-36-2 *S-S* and 2-36-2 *L-L* pulses suggests that the quantum evolution of the system proceeds very differently in these two cases. Changing the CEP of the *S-S* pulse can also modify the picture substantially. In fact, a CEP of 90° makes the 2-36-2 *S-S* pulse look “normal” again.

The partial-wave (ℓ) decomposition of the ionization probability (cf. Fig. 3), when computed after the end of the pulse, is another gauge-invariant parameter that can be used to check the partial-wave convergence of a calculation. In

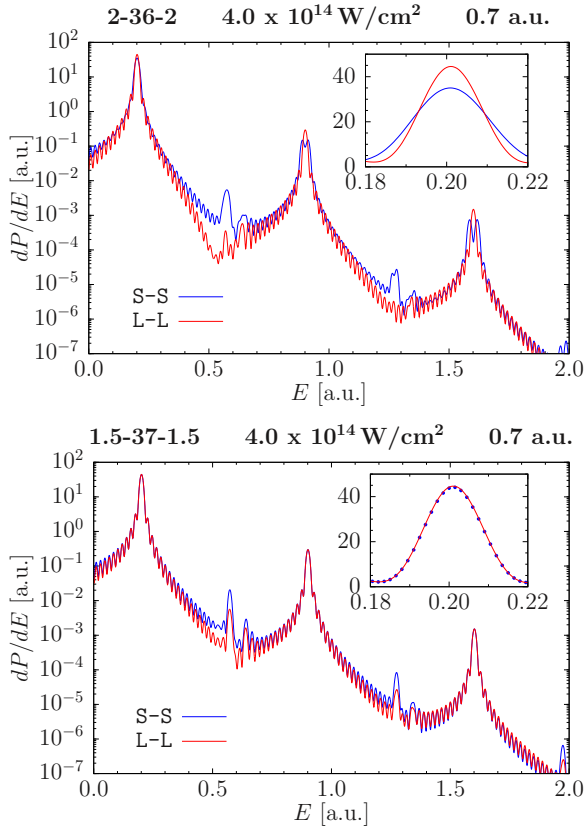


FIG. 2. (Color online) Ejected-electron energy spectrum for hydrogen for the 2-36-2 and 1.5-37-1.5 pulses with central photon energy 0.7 a.u. and peak intensity $4.0 \times 10^{14} \text{ W/cm}^2$. For visibility, dots were used for the S-S results in the lower insert.

practice, the related PAD is measured experimentally, but we first look at the ℓ decomposition.

While the distribution is sharply peaked at $\ell = 1$ for the 2-36-2 L-L pulse, as one would expect for a one-photon process, Figure 3 shows that it is broadly spread out for the 2-36-2 S-S pulse. As demonstrated in Fig. 4, the effect is, indeed, *observable* if the PAD is measured with an *asymmetric energy window* around the central peak. Such windows are typically set in experiments with reaction microscopes [24]. The PADs obtained by integrating differential angle- and energy-resolved ionization probabilities over the energy interval $0.15 \text{ a.u.} \leq E \leq 0.20 \text{ a.u.}$ differ dramatically.

To explain these findings, we resort to the KH picture of the ionization process [25,26]. The Hamiltonian operators \hat{H}_{KH} in the KH gauge and \hat{H}_{V} in the velocity gauge are related by a canonical transformation generated by the operator $\hat{T} = \int_0^t \mathbf{A}(\tau) \cdot \hat{\mathbf{p}} d\tau$, where $\mathbf{A}(\tau)$ is the vector potential. This transformation yields the KH Hamiltonian

$$\hat{H}_{\text{KH}} = e^{i\hat{T}} \hat{H}_{\text{V}} e^{-i\hat{T}} - \frac{\partial \hat{T}}{\partial t} = \frac{\hat{\mathbf{p}}^2}{2} + V(\mathbf{r} + \mathbf{x}(t)), \quad (1)$$

where $\mathbf{x}(t) = \int_0^t \mathbf{A}(\tau) d\tau$, and $V(\mathbf{r})$ is the potential energy in the atomic field-free Hamiltonian displaced by $\mathbf{x}(t)$, which is determined by the classical trajectory launched with initial zero coordinate and velocity in a linearly polarized laser field along the \hat{z} direction. For this geometry $\mathbf{x}(t) = Z_{\text{cl}}(t)\hat{\mathbf{x}}$. The

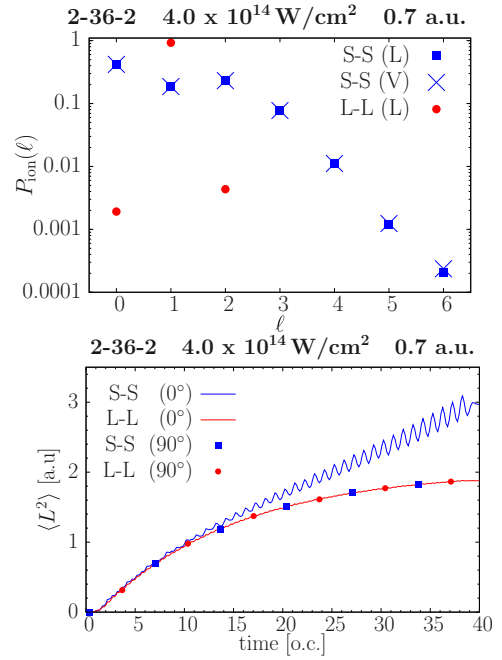


FIG. 3. (Color online) Top: Angular-momentum composition of the ejected-electron wave function after exposure of a hydrogen atom to a 2-36-2 pulse with central photon energy 0.7 a.u. and peak intensity $4.0 \times 10^{14} \text{ W/cm}^2$. Note the broad distribution for the 2-36-2 S-S pulse and the excellent agreement between the numerical predictions obtained by independent computer codes in the length and velocity gauges. Bottom: Quantum mechanical expectation value of $\langle L^2 \rangle$, as a function of time, for CEPs of 0° and 90° . The curve going way from the others after about 10 o.c. is for the 2-36-2 S-S pulse for 0° .

quantity $Z_{\text{cl}}(t)$ is exhibited on the top panel of Fig. 5 for various pulses. It is very different for the 2-36-2 S-S pulse compared to 2-36-2 L-L or either one of the 1.5-37-1.5 pulses.

Changes in $\mathbf{x}(t)$ lead to different KH Hamiltonians. This is illustrated by the KH potential

$$V_{\text{KH}}(\mathbf{r}) = \frac{1}{T_1} \int_0^{T_1} V(\mathbf{r} + \mathbf{x}(t)) dt, \quad (2)$$

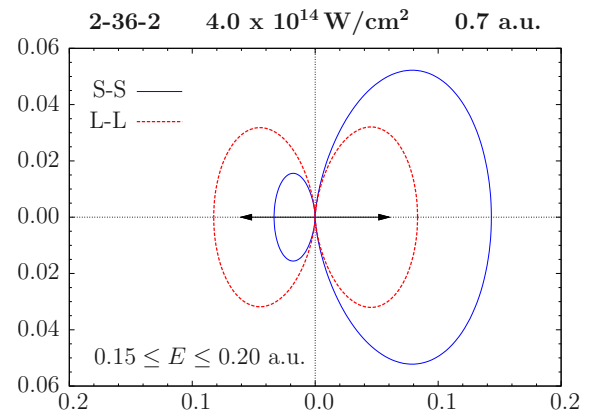


FIG. 4. (Color online) PADs for hydrogen for the 2-36-2 S-S (solid line) and 2-36-2 L-L (dashed line) pulses, integrated over the energy interval 0.15-0.20 a.u. The arrow indicates the direction of the laser polarization axis.

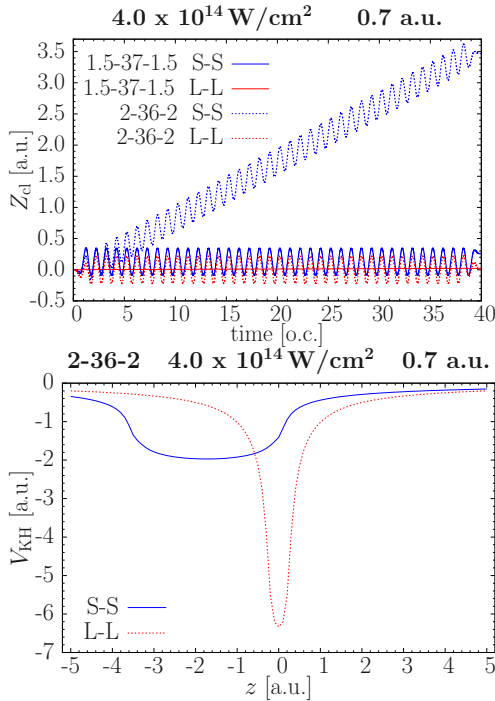


FIG. 5. (Color online) Top: Classical trajectory without Coulomb field for an electron starting at the origin with zero speed under the influence of the laser field for 1.5-37-1.5 and 2-36-2 pulses with central photon energy 0.7 a.u. and peak intensity $4.0 \times 10^{14} \text{W/cm}^2$. The curve going away from the others is for the 2-36-2 *S-S* pulse. Bottom: Kramers-Henneberger potential for the hydrogen atom along the line running at the distance $\rho = 0.1$ a.u. parallel to the laser polarization axis for 2-36-2 *S-S* (solid line) and 2-36-2 *L-L* (dashed line) pulses.

where T_1 is the total pulse duration. $V_{KH}(\mathbf{r})$ represents the zero-order term in the Fourier expansion of the potential $V(\mathbf{r} + \mathbf{x}(t))$. It alone often provides enough information to qualitatively understand the effect of the laser field [12], and corrections can be generated by adding higher-order terms. The bottom panel of Fig. 5 shows $V_{KH}(\mathbf{r})$ for the 2-36-2 *S-S* and 2-36-2 *L-L* pulses. While nearly Coulombic for 2-36-2 *L-L*, $V_{KH}(\mathbf{r})$ is strongly distorted for 2-36-2 *S-S* and far away from a spherically symmetric form. This provides another explanation why the angular-momentum distributions presented above for the 2-36-2 *S-S* case are so broad.

Because of its universal nature, the effect should be observable in any atom or molecule. Indeed, Fig. 6 displays ionization spectra for lithium driven by a similar set of *S-S* and *L-L* pulses. The ramp-on and off effect in the energy spectra is very similar to that observed for hydrogen. It again manifests itself in the PADs integrated over the energy interval covering approximately half of the ionization peak in Fig. 6, while it essentially disappears if a symmetric energy window is used. (cf. Fig. 7).

To summarize, we have demonstrated a significant, and so far unexplored for realistic scenarios, effect of the laser pulse ramp-on and off and CEP on atomic ionization in the strong-field regime for driving XUV pulses with nonzero displacement. We attribute this effect to small changes in the initial conditions launching vastly different classical electron

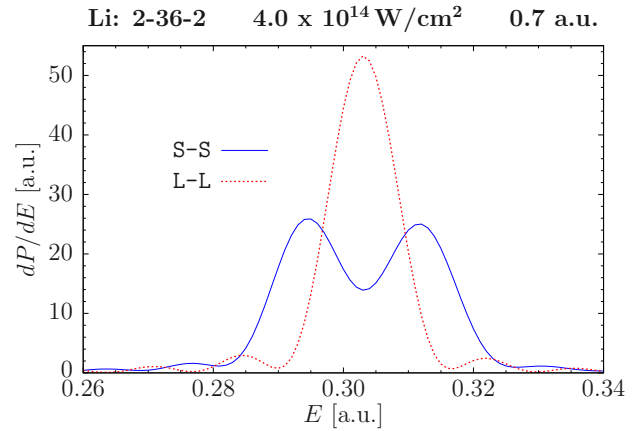


FIG. 6. (Color online) Ejected-electron spectrum for ionization of Li by 2-36-2 *S-S* (solid line) and 2-36-2 *L-L* (dashed line) pulses with central photon energy 0.5 a.u. and peak intensity $4.0 \times 10^{14} \text{W/cm}^2$.

trajectories. The different Kramers-Henneberger potentials experienced by the receding photoelectron result in very diverse photoelectron spectra, angular-momentum compositions, and PADs.

We illustrated the proposed effect using specific pulse parameters that are not far from those presently available from HHG and FEL sources. For combinations of the ramp-on and off and CEP parameters that yield nonzero displacement, we may expect a dramatic effect in the energy spectra and PADs. The stronger the field and the longer the pulse, the more noticeable the effect should generally be. It is also very visible in resonant photoionization, e.g., the Autler-Townes doublet in hydrogen at the resonant photon energy of $3/8$ a.u.

An important issue concerns the occurrence of pulses with a nonzero displacement experimentally. Rastunkov and Krainov [27] strongly favored pulses with zero displacement to prevent the electron from leaving the laser interaction

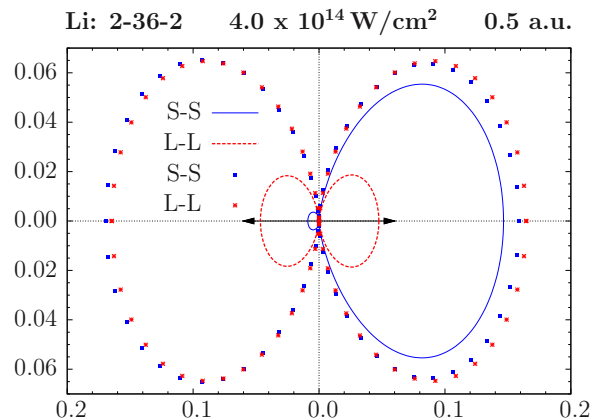


FIG. 7. (Color online) PADs for Li by pulses with central photon energy 0.5 a.u. and peak intensity $4.0 \times 10^{14} \text{W/cm}^2$. Lines are for an asymmetric energy window, $0.25 \text{ a.u.} \leq E \leq 0.30 \text{ a.u.}$, while symbols are for a symmetric energy window, $0.25 \text{ a.u.} \leq E \leq 0.35 \text{ a.u.}$, around the central peak. The arrow indicates the direction of the laser polarization axis.

region too early. In practice, however, a displacement of a few atomic units (cf. Fig. 5) is realistic for typical sizes of the laser focus. The half-cycle pulses obtained in the experiment [28] are examples that not only produce a nonzero displacement, but are also impulsive [29], i.e., they deliver nonzero momentum to a free electron. The same property is demonstrated experimentally for the single-cycle THz pulse [30]. The fact that the shape of these pulses differs from the pulses considered in the present paper is of only secondary importance. Our treatment based on the Kramers-Henneberger picture of the atom-field interaction shows that the effects we observe should manifest themselves for any pulse shape as long as the electron displacement is nonzero.

The authors benefited greatly from stimulating discussions with Peter Hannaford, Misha Ivanov, Igor Litvinyuk, Thomas Pfeifer, Paul Corkum, and Jan-Michael Rost, as well as helpful comments from the referees. K.B. thanks the Australian National University for hospitality. This work was supported by the Australian Research Council under Grant No. DP120101805 (I.A.I. and A.S.K.); by the United States National Science Foundation under Grants No. PHY-1068140 and No. PHY-1430245; the XSEDE allocation PHY-090031 (K.B., J.E., S.M.B.); and by the Russian Foundation for Basic Research under Grant No. 12-02-01123 (E.G. and A.N.G.). Resources of the Australian National Computational Infrastructure (NCI) Facility were also employed.

-
- [1] E. Goulielmakis, M. Schultze, M. Hofstetter, V. S. Yakovlev, J. Gagnon, M. Uiberacker, A. L. Aquila, E. M. Gullikson, D. T. Attwood, R. Kienberger *et al.*, *Science* **320**, 1614 (2008).
- [2] G. Sansone, E. Benedetti, F. Calegari, C. Vozzi, L. Avaldi, R. Flammini, L. Poletto, P. Villoresi, C. Altucci, R. Velotta *et al.*, *Science* **314**, 443 (2006).
- [3] M. Schultze, M. Fiess, N. Karpowicz, J. Gagnon, M. Korbman, M. Hofstetter, S. Neppl, A. L. Cavalieri, Y. Komninos, T. Mercouris *et al.*, *Science* **328**, 1658 (2010).
- [4] K. Klünder, J. M. Dahlström, M. Gisselbrecht, T. Fordell, M. Swoboda, D. Guénot, P. Johnsson, J. Caillat, J. Mauritsson, A. Maquet *et al.*, *Phys. Rev. Lett.* **106**, 143002 (2011).
- [5] W. Ackermann *et al.*, *Nat. Photon.* **1**, 336 (2007).
- [6] T. Shintake *et al.*, *Nat. Photon.* **2**, 555 (2008).
- [7] J. Feldhaus, M. Krikunova, M. Meyer, T. Möller, R. Moshhammer, A. Rudenko, T. Tschentscher, and J. Ullrich, *J. Phys. B* **46**, 164002 (2013).
- [8] P. V. Demekhin and L. S. Cederbaum, *Phys. Rev. Lett.* **108**, 253001 (2012).
- [9] L. Armstrong and S. V. O’Neil, *J. Phys. B* **13**, 1125 (1980).
- [10] C. Cohen-Tannoudji, J. Dupont-Roc, and G. Grynberg, *Atom-Photon Interactions: Basic Processes and Applications* (Wiley, New-York, 2004).
- [11] P. V. Demekhin and L. S. Cederbaum, *Phys. Rev. A* **86**, 063412 (2012).
- [12] F. Morales, M. Richter, S. Patchkovskii, and O. Smirnova, *Proc. Natl. Acad. Sci.* **108**, 16906 (2011).
- [13] K. Toyota, U. Saalman, and J. M. Rost, [arXiv:1408.4541](https://arxiv.org/abs/1408.4541).
- [14] A. L. Nefedov, *Phys. Rev. A* **50**, R903 (1994).
- [15] N. J. Kylstra, R. A. Worthington, A. Patel, P. L. Knight, J. R. Vazquez de Aldana, and L. Roso, *Phys. Rev. Lett.* **85**, 1835 (2000).
- [16] J. Crank and P. Nicolson, *Adv. Comput. Math.* **6**, 207 (1996).
- [17] M. Nurhuda and F. H. M. Faisal, *Phys. Rev. A* **60**, 3125 (1999).
- [18] T. Park and J. Light, *J. Chem. Phys.* **85**, 5870 (1986).
- [19] M. G. Pullen, W. C. Wallace, D. E. Laban, A. J. Palmer, G. F. Hanne, A. N. Grum-Grzhimailo, K. Bartschat, I. Ivanov, A. Kheifets, D. Wells *et al.*, *Phys. Rev. A* **87**, 053411 (2013).
- [20] O. Graydon, *Nat. Photon.* **7**, 585 (2013).
- [21] M. Schuricke, G. Zhu, J. Steinmann, K. Simeonidis, I. Ivanov, A. Kheifets, A. N. Grum-Grzhimailo, K. Bartschat, A. Dorn, and J. Ullrich, *Phys. Rev. A* **83**, 023413 (2011).
- [22] H. M. Tetchou Nganso, Yu. V. Popov, B. Piraux, J. Madroñero, and M. G. Kwato Njock, *Phys. Rev. A* **83**, 013401 (2011).
- [23] A. N. Grum-Grzhimailo, M. N. Khaerdinov, and K. Bartschat, *Phys. Rev. A* **88**, 055401 (2013).
- [24] J. Ullrich, R. Moshhammer, A. Dorn, R. Dörner, L. P. H. Schmidt, and H. Schmidt-Böcking, *Rep. Prog. Phys.* **66**, 1463 (2003).
- [25] H. A. Kramers, *Collected Scientific Papers* (North Holland, Amsterdam, 1956).
- [26] W. C. Henneberger, *Phys. Rev. Lett.* **21**, 838 (1968).
- [27] V. S. Rastunkov and V. P. Krainov, *J. Phys. B* **40**, 2277 (2007).
- [28] H.-C. Wu and J. Meyer-ter-Vehn, *Nat. Photon.* **6**, 304 (2012).
- [29] E. Persson, K. Schiessl, A. Scrinzi, and J. Burgdörfer, *Phys. Rev. A* **74**, 013818 (2006).
- [30] S. Li and R. R. Jones, *Phys. Rev. Lett.* **112**, 143006 (2014).